



Published in final edited form as:

J Immunol. 2015 June 15; 194(12): 5736–5742. doi:10.4049/jimmunol.1401986.

Exacerbated Experimental Colitis In TNFAIP8-deficient Mice

Honghong Sun^{1,4}, Yunwei Lou^{1,2,4}, Thomas Porturas¹, Samantha Morrissey¹, George Luo¹, Ji Qi¹, Qingguo Ruan¹, Songlin Shi^{1,3}, and Youhai H. Chen^{1,5}

¹Department of Pathology and Laboratory Medicine, University of Pennsylvania Perelman School of Medicine, Philadelphia, PA, 19104, USA.

²Department of Immunology, Shandong University School of Medicine, Ji'nan, P. R. China.

³Xiamen University School of Medicine, Ximen, P. R. China.

Abstract

The TNF- α -induced protein 8 (TNFAIP8 or TIPE) is a risk factor for cancer and bacterial infection, and its expression is upregulated in a number of human cancers. However, its physiological and pathological functions are unclear. We describe here the generation of TIPE-deficient mice and their increased sensitivity to colonic inflammation. TIPE-deficient mice were generated by germ line gene targeting and were born without noticeable developmental abnormalities. Their major organs including lymphoid organs and intestines were macroscopically and microscopically normal. However, after drinking dextran sodium sulfate-containing water, TIPE-deficient mice developed more severe colitis than wild type mice, as demonstrated by decreased survival rates, increased body weight loss, and enhanced leukocyte infiltration, bacterial invasion, and inflammatory cytokine production in the colon. Bone marrow chimeric experiments revealed that TIPE deficiency in non-hematopoietic cells was responsible for the exacerbated colitis in TIPE-deficient mice. Consistent with this result, TIPE-deficient intestinal epithelial cells had increased rate of cell death and decreased rate of proliferation as compared to wild type controls. Taken together, these findings indicate that TIPE plays an important role in maintaining colon homeostasis and in protecting against colitis.

Keywords

Colitis; Inflammation; Cell death; TNFAIP8 (TIPE)

Introduction

TNF- α -induced protein 8 (TNFAIP8 or TIPE), also known as SCC-S2, GG2-1, NDED, and MDC-3.13, is the first member of the TNFAIP8 family that was cloned and studied (1–4). TIPE may prevent apoptosis in certain tumor cell lines and increase their oncogenic potential (1, 2). Overexpression of *TIPE* gene in tumor cells correlates with enhanced

⁵Corresponding Author: Youhai H. Chen, M.D., Ph.D., Department of Pathology and Laboratory Medicine, University of Pennsylvania Perelman School of Medicine, 713 Stellar-Chance Labs, 422 Curie Blvd., Philadelphia, PA 19104-6160. Phone: 215 898 4671. FAX: 215 573 3434. yhc@mail.med.upenn.edu.

⁴These authors contributed equally to this work.

proliferation and tumorigenicity (5). By contrast, TIPE may promote glucocorticoid-induced apoptosis of normal thymocytes in culture (6). TIPE has been reported to interact with activated Gαi to regulate cell death and transformation, and to interact with karyopherin alpha2 in PC-3 cells (7). *TIPE* gene polymorphism or over-expression is associated with susceptibility to *Staphylococcus aureus* infection (8), cancer development (9–11), and psoriasis (12). TIPE may not only be involved in disease pathogenesis, but also serve as a biomarker for certain inflammatory and neoplastic diseases. However, the precise roles of TIPE in health and disease remain to be established.

Human inflammatory bowel diseases (IBD), including ulcerative colitis and Crohn's disease, are a major health problem in developed countries (13). These diseases are characterized by chronic colonic inflammation and are mediated by infiltrating inflammatory cells. The etiologic factors that trigger these diseases are not well understood. In mice, oral administration of dextran sodium sulfate (DSS) induces a form of colitis that shares many pathological and clinical features with human inflammatory bowel diseases; therefore DSS-induced colitis is considered to be a valuable experimental model for human inflammatory bowel diseases (14–16).

Increased colon epithelial cell death and decreased proliferation are associated with the development of colitis. Given the potential roles of TIPE in regulating these processes, we set out to test the *in vivo* effect of TIPE deficiency on the development of DSS-induced colitis using our newly generated *Tipe*-deficient mice. Our data indicate that TIPE plays a crucial role in maintaining colonic homeostasis during colitis.

Materials and Methods

Animals

Wild type (WT) C57BL/6 (B6) and CD45.1⁺ B6 mice were purchased from The Jackson Laboratory. All mice used in this study were housed under pathogen-free conditions in the University of Pennsylvania Animal Care Facilities. All animal protocols used were pre-approved by the Institutional Animal Care and Use Committee of the University of Pennsylvania.

Generation and Genotyping of *Tipe*^{-/-} Mice

The B6 ES cell line with a disrupted *Tipe* gene (NM_134131) was obtained from the Texas A&M Institute for Genomic Medicine (College Station, Texas). The gene-trapping vector that disrupts *Tipe* gene was inserted into the only intron of the gene. The ES cells were injected into mouse blastocysts to generate chimeras. Six chimeras, one female and five males, were produced. The germline transmission was obtained from one of the male chimeras. A common WT primer 1 (5'-CCAAAGGCTCAACATGCTCT-3') was paired with (i) a reverse primer 3 (5'-CCAATAAACCCCTCTTGCAGTTGC-3') against the sequence on gene trap vector to produce a 190 bp PCR fragment from *Tipe*-deficient allele, and (ii) a WT reverse primer 2 (5'-CCCATGTGTGCAAGTGAAAA-3') to generate a 334 bp PCR fragment from the wild type allele. Heterozygous mice for the disrupted *Tipe* locus were bred to produce homozygous *Tipe*^{-/-} animals. Once identified, they were further tested

by PCR using primers 4 (5'-ACCTGGCCGTTTCAGGCACAA-3') and primer 5 (5'-TCACCCTGTACAGCTCATCT-3') to ensure that *Tipe* mRNA is not expressed in *Tipe*^{-/-} animals.

RT-PCR

Total RNA was isolated from brain, spinal cord, lung, liver, heart, spleen, intestine, and mesenteric lymph nodes of both wild type and *Tipe*^{-/-} mice with Trizol reagent (Sigma) according to the manufacturer's instruction. The isolated RNA was further purified with RNeasy Mini kits (Qiagen) according to the manufacturer's instruction. 250 ng of RNA samples were reversely transcribed with oligo(dT) and SuperScript II transcriptase (Invitrogen). The generated cDNA was diluted with sterile Milli-Q water (1:4). Real-time quantitative PCR analysis was performed using specific Quantitect Primers for mouse GAPDH, *TIPE*, *TIPE1*, *TIPE2*, *TIPE3*, *IL-6*, *IL-1β*, *IL-17*, and *CXCL2* (Qiagen) in an Applied Biosystems 7500 system using Power SYBR Green PCR Master Mix (Applied Biosystems). Relative levels of gene expression were determined with GAPDH as the control.

DSS-Induced Colitis

Experimental colitis was induced with 3% or 4% (w/v) DSS (MW 36,000–50,000; MP Biologicals) dissolved in sterile, distilled water ad libitum for five days followed by normal drinking water until the end of experiment. For survival studies, eight-to-ten weeks old mice were treated with 4% DSS for five days and replaced with normal drinking water until day 14. For histology, gene expression and cytokine production studies, mice were treated with 3% DSS for five days followed by regular drinking water for two days and euthanized at different time points after the DSS treatment.

Determination of Clinical Scores

Body weight, stool consistency, and rectal bleeding were monitored daily (17). In brief, stool scores were determined as follows: 0, well-formed pellets; 1, soft and semiformed but not adhered to the anus; 2, semiformed but adhered to the anus; 4, liquid stool. Bleeding scores were determined as follows: 0, no blood; 1, blood traces in rectum; 2, visible blood in whole rectum; 4, gross rectal bleeding. Weight loss scores were monitored as follows: 0, no body weight change; 1, body weight loss within 5%; 2, body weight loss within 10%; 3, weight loss within 20%; 4, Body weight loss exceeds 20%. DAI (disease activity index) was the total sum of these 3 scores.

Histopathology and Immunohistochemistry

The entire colon was excised to measure the length. The distal colons were washed, fixed in 10% buffered formalin and embedded in paraffin. Tissue sections were stained with hematoxylin & eosin (H&E). For Ki-67 and active caspase 3 staining, mice were treated with DSS and colons were collected, washed, and fixed in 10% formalin. Colon sections were then stained with Ki-67 and active caspase 3 antibody (R&D Systems). For TUNEL, slides were deparaffinized and rehydrated, and then treated with proteinase K (DAKO S3004) for 20 min at 40°C. Slides were then rinsed in Tris buffer, incubated with the Roche

enzyme labeling mix for 60 min at 40°C, counterstained with DAPI, and mounted with Prolong Gold (Lifetechnologies P36934). TUNEL slides were scanned on an FL slide scanner (Leica Bioimaging) and images were analyzed using the Cyto-nuclear FL v1.3 algorithm (Indica Labs).

Bone Marrow Chimeras

Bone marrow cells were flushed from the femurs and tibias of donor mice. The red blood cells were lysed with ACK solution (8.29g NH₄Cl, 1g KHCO₃, 37.2mg Na₂EDTA in 1L of water). Cells were washed twice and re-suspended in cold PBS. Recipient mice were lethally irradiated with 500 rads twice separated by 4 hours. The irradiated mice received a total of 10×10⁶ of donor bone marrow cells by tail vein injection one or two hours after irradiation. Six to seven weeks later, peripheral blood leukocytes were collected and stained with CD45.1 and CD45.2 antibodies to determine the reconstitution rate. In the chimeric mice so generated, more than 90% of the hematopoietic cells were derived from donor bone marrow (18).

Isolation of Colon Epithelial Cells

Colonic epithelial cells were isolated as described (19, 20). In brief, colons were dissected, washed with cold PBS, and cut into small pieces. Colon segments were incubated in PBS supplemented with 1mM EDTA and 1mM DTT for 30min at 37°C with gentle shaking. Cells in supernatants were filtered through a 70 µm cell strainer and washed twice. Enrichment for colonic epithelial cells was confirmed by staining cells for the epithelial cell-specific marker EpCam (eBioscience). 70–80% of isolated cells stained positive for EpCam. If needed, the isolated colonic epithelial cells were cultured in epithelial cell culture medium (ECM) containing equal volumes of phenol-red-free DMEM and Ham's F-12 medium (Biowhittaker) with the following additives: 5 µg of insulin (Sigma)/ml, 5×10⁸ M dexamethasone (Sigma), 60 nM selenium (Sigma), 5×10⁸ M triiodothyrenine (Sigma), 5 µg of transferrin (Sigma)/ml, 10 ng of Eidermal growth factor (Sigma)/ml, 20 mM HEPES, 2 mM glutamine, 10% Penicillin/streptomycin, and 2% FBS.

Colon leukocytes isolation

Colon leukocytes were isolated using a modified version of a previously described protocol (21). Briefly, colon was washed 3 times and incubated in PBS with 5% FBS, 2mM EDTA, 1mM DTT for 15 min at 37°C with shaking (250 RPM). This was repeated 3 times to remove epithelial cells. The colon samples without epithelial cells were digested in PBS with 5% FBS, 0.5 mg/ml collagenase (Sigma), 0.02 mg/ml Dnase (Roche), and 0.1 mg/ml Dispase (Invitrogen), for 20 minutes at 37°C with gentle shaking for another 45 min with shaking at 37°C. The mixture then was filtered through 70 µm cell strainer. The flow through contains colon leukocytes.

Plasmid DNA transfection and viral infection

293T cells were transfected with plasmid DNA using Fugene 6 (Promega) reagent according to the manufacturer's instructions. For virus production, pLKO.1 (with puromycin resistance) with shRNA-Tnfaip8 (purchased from Open Biosystems) or shScr (purchased

from Addgene) fragments and packaging constructs were co-transfected into 293T cells. After 24 and 48 hrs, virus-containing medium was filtered and used to infect 3T3 cell lines in the presence of 6.5 mg/ml of polybrene (Millipore). Infected cells were selected using puromycin (Sigma) to establish shRNA-Scr, shRNA-Tnfaip8-1, and shRNA-Tnfaip8-2 cell lines. Viral vectors were produced from the pLKO.1 plasmid containing shRNA-Tnfaip8-1 (AAAGGGATTGTACAAGGCAGC), shRNA-Tnfaip8-2 (TTGAACTGATTGTTCTGTGG), or shRNA-scr (CGAGGGCGACTTAACCTTAGG). The shRNA-Tnfaip8-1 knockdown all Tipe protein expression.

ELISA

The colon homogenates and serum were collected and stored at -80°C . Antibodies used in ELISA were purchased from BD Pharmingen and eBioscience including purified and biotinylated rat anti-mouse IL-6, IL-17A, and IL-1 β . Quantitative ELISA was performed using paired mAbs specific for the corresponding cytokines according to the manufacturer's instruction.

Phenotyping of *Tipe*^{-/-} Mice

Six-to-eight-week age-matched WT and knockout mice were sacrificed and their immune organs collected and weighted. Single cell suspensions were prepared, and total cell numbers from each organ were determined using the COULTER Counter (Beckman). Flow cytometry was performed after staining cells with anti-mouse CD4, CD8, B220, Gr-1, CD11b, CD11c, NK1.1, CD25, CD44, Foxp3, CD62L, and CD69. All the antibodies used were purchased from BD Bioscience.

Bacterial culture

Colon samples were collected and processed as described above, and then homogenized in CelLytic™ M buffer (Sigma) and serially diluted. Different dilutions of the tissue homogenates were plated in triplicates on blood agar (BD Bioscience) and BHI agar. The bacterial colonies formed were counted after incubating at 37°C for 24 hrs.

Cell death and proliferation

Colon samples were processed and epithelial cells were obtained from control and colitis WT and *Tipe*^{-/-} mice. The isolated epithelial cells were collected and the cell death was determined by 7AAD and Annexin V staining. Alternatively, *Tipe* knockdown 3T3 cells were treated with 3% DSS for 16 hrs and the cells were harvested for 7AAD and Annexin V staining. The in situ colonocyte proliferation was assessed by Ki67 staining and cell death was determined by active caspase 3 and TUNEL staining after the colon tissues were collected from DSS-treated mice and fixed in 10% buffered formalin and embedded in paraffin.

Blood cell counts

Blood was collected retro-orbitally and whole blood cell counts were determined using Drew Hemavet 950FS (Drew Scientific, Oxford, U.K.).

Statistical analysis

Quantitative data are presented as means±SEM of two or three experiments. The survival curves were plotted according to the Kaplan-Meier method and compared by the log-rank test. Mann-Whitney U test was used to compare the body weight data. Two-tailed Student *t* test was used for all other cases and *p*<0.05 was considered statistically significant. All statistical analyses were performed with the Prism Software.

Results

Generation and Phenotyping of *Tipe*-deficient Mice

Tipe^{-/-} mice were generated using gene trap technology to target *Tipe* gene in B6 ES cells. The gene-trapping vector is composed of a LTR (viral long terminal repeat), a splice acceptor site, a Neomycin-resistant gene, and a polyA tail that stops *Tipe* gene transcription (Figure 1A). This disrupted *Tipe* gene allele results in a complete loss of the short isoform of *Tipe* mRNA and a truncated long isoform of *Tipe* mRNA that encodes the first N-terminal 24 amino acids. Homozygous offsprings were identified by PCR (Figure 1B). They were further tested to ensure the lack of the full-length *Tipe* mRNA in a variety of organs (Figure 1C).

Tipe gene mutation did not affect the gross growth and development of mice. Homozygous *Tipe*^{-/-} mice were born with the expected Mendelian ratios with no detectable developmental abnormalities. The weight, structure, and cellular compositions of lymphoid organs are normal (Supplemental Figures 1, 2A–2C) in *Tipe*^{-/-} mice. Downregulation of TIPE was reported to protect thymocytes against glucocorticoid-mediated apoptosis. However, no significant differences between WT and *Tipe*^{-/-} groups were detected in thymocyte death induced by dexamethasone (Supplemental Figure 2D).

Tipe^{-/-} Mice Are Hyper-sensitive to DSS-induced Colitis

Tipe^{-/-} mice did not appear to develop more spontaneous diseases than WT littermates. However, after drinking DSS-containing water, despite similar amount of water consumption (Supplemental Figure 3), they developed more severe colitis than WT mice. They began to die on day six after the DSS treatment. By day ten, all of the *Tipe*^{-/-} animals had died while 40% of WT animals were still alive (Figure 2A). The *Tipe*^{-/-} mice suffered greater body weight loss (Figure 2B) and increased overall disease manifestations (Figure 2C). To further assess the severity of colitis, colon length was also measured. The DSS-fed *Tipe*^{-/-} mice had significantly shorter and lighter colons (Figure 2D–F). Consistent with these findings, a histopathological examination of H&E-stained colons of knockout mice revealed more severe colitis characterized by crypt loss and infiltrating leukocytes than in the controls (Figure 2G).

Enhanced Inflammatory Responses in *Tipe*^{-/-} Mice with Colitis

To further identify the roles of TIPE in DSS-induced colitis, we examined the hematological and immunological aspects of the disease in age- and sex-matched *Tipe*^{-/-} mice and WT controls. As shown in Figure 3A, significantly increased neutrophil counts were detected in *Tipe*^{-/-} blood samples. At the same time, the spleens of *Tipe*^{-/-} mice became smaller

(Figure 3B) while more leukocytes were found in the colon of these mice (Figure 3C and 3D). Enhanced levels of IL-17A and IL-6 were also found in the sera of *Tipe*^{-/-} mice (Figure 4A). Similarly, enhanced levels of IL-6, IL-17A, and IL-1 β proteins (Figure 4B) and/or mRNAs (Figure 4C) were detected in the *Tipe*^{-/-} colons. Increased CXCL2 mRNA expression was also detected in *Tipe*^{-/-} colons (Figure 4C). These observations point to enhanced inflammatory responses in the *Tipe*^{-/-} colon after DSS treatment.

TIPE-deficiency in Non-hematopoietic Cells Exacerbates Colitis

Although enhanced inflammatory responses were detected in the DSS-challenged *Tipe*^{-/-} mice, both hematopoietic and non-hematopoietic compartments could contribute to the exacerbated colitis phenotype observed above. To assess which compartment contributes directly to the exacerbation of colitis in *Tipe*^{-/-} mice, we reconstituted lethally irradiated WT and *Tipe*^{-/-} mice with bone marrow cells from WT or *Tipe*^{-/-} mice. After recovering for eight weeks, mice were then subjected to five days of DSS treatment followed by two days of normal drinking water. As shown in Figure 5, after DSS treatment, the WT mice receiving wild type or *Tipe*^{-/-} bone marrow cells demonstrated similar changes in body weight, disease index, and colon length (Figure 5, A, B, and C) indicating that hematopoietic cells are not major contributors to the exacerbation of colitis observed in *Tipe*^{-/-} mice. By contrast, when WT bone marrow cells were injected into *Tipe*^{-/-} or WT recipient mice, after DSS treatment, *Tipe*^{-/-} recipients developed more severe colitis than the WT recipients indicating that the non-hematopoietic compartment plays a major role in the disease exacerbation (Figure 5, A, B, and C).

Increased Bacterial Invasion of the Colonic Tissue in TIPE-deficient Mice

The disruption of mucosal barrier following gastrointestinal epithelial cell injury can lead to commensal bacterial infection and potent inflammatory responses against them, which is believed to be part of the pathogenic mechanisms of DSS-induced colitis (22–24). We next checked bacterial numbers in the colons of WT and *Tipe*^{-/-} mice with colitis. We found significantly more bacteria in the colons of *Tipe*^{-/-} mice (Figure 6) than in WT mice, indicating enhanced dissemination of the commensal bacteria.

TIPE-deficiency in Epithelial Cells Affects Their Survival and Proliferation

TIPE is expressed in a large number of cell types including colonic epithelial cells (Supplemental Figure 4). The increased mortality in *Tipe*^{-/-} mice could be explained by increased cell death and/or decreased proliferation of colonic epithelial cells during colitis (25). To test whether TIPE-deficiency affects epithelial cell death and proliferation, epithelial cells were isolated from normal and DSS-fed WT and TIPE-deficient colons and the cell death was determined by 7-AAD and Annexin V staining. Live epithelial cells were 7-AAD and Annexin V double negative cells (Figure 7A). Increased cell death was detected in the *Tipe*^{-/-} group as compared to WT controls. PI3K-AKT pathway is important for regulating cell death and immunity (26). A significantly reduced level of activated AKT was detected in the *Tipe*^{-/-} colon samples, indicating that the increased cell death might be due to the downregulation of the PI3K-AKT signaling (Figure 7B). Consistent with these findings, TIPE knockdown in the NIH3T3 cell line significantly increased cell death induced

by 3% DSS (Figure 7C). Ki67 is an endogenous marker for cell proliferation. Significantly reduced Ki67 staining (Figure 7, D and E) was found in DSS-fed *Tipe*^{-/-} colons compared to those of the WT, suggesting that TIPE protein is required for epithelial cell proliferation after DSS-induced colon damage. Significantly increased active caspase 3 staining and TUNEL staining (Figure 7F-I) were also observed in the *Tipe*^{-/-} colons, demonstrating augmented cell death. Taking together, increased death of *Tipe*^{-/-} epithelial cells, combined with compromised proliferation, may be responsible for the increased mortality in TIPE-deficient mice treated with DSS.

Discussion

In the present study, we generated TIPE-deficient mice and studied TIPE's role in development and DSS-induced colitis. We showed that *Tipe*^{-/-} mice were significantly more susceptible to DSS-induced colitis and the loss of TIPE expression in non-hematopoietic compartment played a major role. The knockout mice suffered from a greater body weight loss, more severe diarrhea and rectal bleeding, and enhanced mortality, indicating a key role for TIPE in protecting against DSS-induced colon damage.

TIPE has been reported as an anti-apoptotic molecule in tumor cells (5) but knocking down its expression by RNAi protects thymocytes from glucocorticoid-mediated apoptosis (6). Although we did not observe significant differences in apoptosis between knockout immune cells and WT controls under physiological conditions, increased cell death was observed in *Tipe*^{-/-} epithelial cells under inflamed condition, indicating an important role for TIPE protein in inflammatory diseases.

The mammalian TIPE family consists of four members: TIPE, TIPE1, TIPE2, and TIPE3, which are highly conserved in their amino acid sequences. TIPE2 regulates the function of the innate immune system by targeting PI3K-AKT-Rac axis (26) whereas TIPE3 promotes AKT activation by acting as a PtdIns(4,5)*P*₂ and PtdIns(3,4,5)*P*₃ transfer protein (27). In this study, we found decreased AKT activity in *Tipe* knockout colon, indicating that *Tipe* may regulate epithelial cell death by targeting AKT. PI3-kinase generates PtdIns(3,4,5)*P*₃, which in turn activates AKT. AKT is a serine/threonine protein kinase with oncogenic and antiapoptotic activities. It phosphorylates a number of proteins, including cell death regulators such as BAD, CREB, MDM2, and NF- κ B, leading to diminished cell death. PI3K p110 δ mutant mice of the C57BL/6 background develop spontaneous colitis (28), and AKT1-deficient mice of the 129 background have increased sensitivity to DSS-induced colitis (29). Additionally, protein kinase-R (PKR)-deficient mice develop more severe clinical and histological manifestations of DSS-induced colitis likely due to reduced activation of STAT3 and AKT (30). Therefore, the roles of AKT in the death of *Tipe*-deficient epithelial cells during colitis need to be further studied.

The epithelial barrier integrity in gastrointestinal system is crucial for protecting against environmental insults, including toxins, antigens, and microbes (31). Increased epithelial cell death and decreased proliferation are associated with DSS-induced colitis (20, 32, 33). In our study, we showed that the loss of epithelial integrity caused by increased epithelial cell death in TIPE knockout mice may lead to increased dissemination of commensal

bacteria and enhanced leukocyte infiltration and inflammatory responses. Inflammation is closely linked to the development of cancer. TIPE dysregulation is associated with the development of a number of human cancers. Results reported here may also help advance our understanding of the pathogenic mechanisms of cancer. Besides its function in cell death and proliferation, TIPE may also play a role in cell migration and metastasis. The knockout mice described here provide a useful tool to study the broad biology of the TIPE protein in health and disease.

Supplementary Material

Refer to Web version on PubMed Central for supplementary material.

Acknowledgements

The authors thank Drs. Jean Richa, Ping Jiang, and members of the Transgenic Cores of the University of Pennsylvania and Wistar Institute for technical supports in generating TIPE-deficient mice, and the Pathology Core at Children's Hospital of Philadelphia for H&E and immunohistological staining. We also thank Drs. Terry Cathopoulos, Derek Johnson, Xiaohong Liang, Svetlana Fayngerts, and George Buchlis for reagents and/or valuable advice.

This work was funded by National Institutes of Health, USA (AI-077533, AI-050059, and GM-085112 to YHC). Y.L. is supported by a fellowship from the China Scholarship Council (No. 201206220065).

References

1. Kumar D, Whiteside TL, Kasid U. Identification of a novel tumor necrosis factor- α -inducible gene, SCC-S2, containing the consensus sequence of a death effector domain of fas-associated death domain-like interleukin-1 β -converting enzyme-inhibitory protein. *J Biol Chem.* 2000; 275:2973–2978. [PubMed: 10644768]
2. Zhang C, Chakravarty D, Sakabe I, Mewani RR, Boudreau HE, Kumar D, Ahmad I, Kasid UN. Role of SCC-S2 in experimental metastasis and modulation of VEGFR-2, MMP-1, and MMP-9 expression. *Mol Ther.* 2006; 13:947–955. [PubMed: 16455304]
3. Sun H, Gong S, Carmody RJ, Hilliard A, Li L, Sun J, Kong L, Xu L, Hilliard B, Hu S, Shen H, Yang X, Chen YH. TIPE2, a negative regulator of innate and adaptive immunity that maintains immune homeostasis. *Cell.* 2008; 133:415–426. [PubMed: 18455983]
4. Lou Y, Liu S. The TIPE (TNFAIP8) family in inflammation, immunity, and cancer. *Mol Immunol.* 2011; 49:4–7. [PubMed: 21924498]
5. Kumar D, Gokhale P, Broustas C, Chakravarty D, Ahmad I, Kasid U. Expression of SCC-S2, an antiapoptotic molecule, correlates with enhanced proliferation and tumorigenicity of MDA-MB 435 cells. *Oncogene.* 2004; 23:612–616. [PubMed: 14724590]
6. Woodward MJ, de Boer J, Heidorn S, Hubank M, Kioussis D, Williams O, Brady HJ. Tnfaip8 is an essential gene for the regulation of glucocorticoid-mediated apoptosis of thymocytes. *Cell Death Differ.* 2010; 17:316–323. [PubMed: 19730441]
7. Laliberte B, Wilson AM, Nafisi H, Mao H, Zhou YY, Daigle M, Albert PR. TNFAIP8: a new effector for Galpha(i) coupling to reduce cell death and induce cell transformation. *J Cell Physiol.* 2010; 225:865–874. [PubMed: 20607800]
8. Ahn SH, Deshmukh H, Johnson N, Cowell LG, Rude TH, Scott WK, Nelson CL, Zaas AK, Marchuk DA, Keum S, Lamlerthton S, Sharma-Kuinkel BK, Sempowski GD, Fowler VG Jr. Two genes on A/J chromosome 18 are associated with susceptibility to *Staphylococcus aureus* infection by combined microarray and QTL analyses. *PLoS Pathog.* 2010; 6:e1001088. [PubMed: 20824097]
9. Liu T, Gao H, Chen X, Lou G, Gu L, Yang M, Xia B, Yin H. TNFAIP8 as a predictor of metastasis and a novel prognostic biomarker in patients with epithelial ovarian cancer. *Br J Cancer.* 2013; 109:1685–1692. [PubMed: 23982604]

10. Romanuik TL, Ueda T, Le N, Haile S, Yong TM, Thomson T, Vessella RL, Sadar MD. Novel biomarkers for prostate cancer including noncoding transcripts. *Am J Pathol.* 2009; 175:2264–2276. [PubMed: 19893039]
11. Shi TY, Cheng X, Yu KD, Sun MH, Shao ZM, Wang MY, Zhu ML, He J, Li QX, Chen XJ, Zhou XY, Wu X, Wei Q. Functional variants in TNFAIP8 associated with cervical cancer susceptibility and clinical outcomes. *Carcinogenesis.* 2013; 34:770–778. [PubMed: 23299407]
12. Filkork K, Hegedus Z, Szasz A, Tubak V, Kemeny L, Kondorosi E, Nagy I. Genome wide transcriptome analysis of dendritic cells identifies genes with altered expression in psoriasis. *PLoS One.* 2013; 8:e73435. [PubMed: 24039940]
13. Fiocchi C. Inflammatory bowel disease: etiology and pathogenesis. *Gastroenterology.* 1998; 115:182–205. [PubMed: 9649475]
14. Perse M, Cerar A. Dextran sodium sulphate colitis mouse model: traps and tricks. *J Biomed Biotechnol.* 2012; 2012:718617. [PubMed: 22665990]
15. Strober W, Fuss I, Mannon P. The fundamental basis of inflammatory bowel disease. *J Clin Invest.* 2007; 117:514–521. [PubMed: 17332878]
16. Diaz-Granados N, Howe K, Lu J, McKay DM. Dextran sulfate sodium-induced colonic histopathology, but not altered epithelial ion transport, is reduced by inhibition of phosphodiesterase activity. *Am J Pathol.* 2000; 156:2169–2177. [PubMed: 10854237]
17. Castaneda FE, Walia B, Vijay-Kumar M, Patel NR, Roser S, Kolachala VL, Rojas M, Wang L, Oprea G, Garg P, Gewirtz AT, Roman J, Merlin D, Sitaraman SV. Targeted deletion of metalloproteinase 9 attenuates experimental colitis in mice: central role of epithelial-derived MMP. *Gastroenterology.* 2005; 129:1991–2008. [PubMed: 16344067]
18. Hilliard BA, Mason N, Xu L, Sun J, Lamhamedi-Cherradi SE, Liou HC, Hunter C, Chen YH. Critical roles of c-Rel in autoimmune inflammation and helper T cell differentiation. *J Clin Invest.* 2002; 110:843–850. [PubMed: 12235116]
19. Reynolds JM, Martinez GJ, Nallaparaju KC, Chang SH, Wang YH, Dong C. Cutting edge: regulation of intestinal inflammation and barrier function by IL-17C. *J Immunol.* 2012; 189:4226–4230. [PubMed: 23024280]
20. Zaki MH, Boyd KL, Vogel P, Kastan MB, Lamkanfi M, Kanneganti TD. The NLRP3 inflammasome protects against loss of epithelial integrity and mortality during experimental colitis. *Immunity.* 2010; 32:379–391. [PubMed: 20303296]
21. Drakes ML, Czinn SJ, Blanchard TG. Isolation and purification of colon lamina propria dendritic cells from mice with colitis. *Cytotechnology.* 2004; 46:151–161. [PubMed: 19003269]
22. Brown EM, Sadarangani M, Finlay BB. The role of the immune system in governing host-microbe interactions in the intestine. *Nat Immunol.* 2013; 14:660–667. [PubMed: 23778793]
23. Brestoff JR, Artis D. Commensal bacteria at the interface of host metabolism and the immune system. *Nat Immunol.* 2013; 14:676–684. [PubMed: 23778795]
24. Honda K, Littman DR. The microbiome in infectious disease and inflammation. *Annu Rev Immunol.* 2012; 30:759–795. [PubMed: 22224764]
25. Araki Y, Mukaisyo K, Sugihara H, Fujiyama Y, Hattori T. Increased apoptosis and decreased proliferation of colonic epithelium in dextran sulfate sodium-induced colitis in mice. *Oncol Rep.* 2010; 24:869–874. [PubMed: 20811666]
26. Sun H, Zhuang G, Chai L, Wang Z, Johnson D, Ma Y, Chen YH. TIPE2 controls innate immunity to RNA by targeting the phosphatidylinositol 3-kinase-Rac pathway. *J Immunol.* 2012; 189:2768–2773. [PubMed: 22904303]
27. Fayngerts SA, Wu J, Oxley CL, Liu X, Vourekas A, Cathopoulos T, Wang Z, Cui J, Liu S, Sun H, Lemmon MA, Zhang L, Shi Y, Chen YH. TIPE3 Is the Transfer Protein of Lipid Second Messengers that Promote Cancer. *Cancer Cell.* 2014; 26:465–478. [PubMed: 25242044]
28. Uno JK, Rao KN, Matsuoka K, Sheikh SZ, Kobayashi T, Li F, Steinbach EC, Sepulveda AR, Vanhaesebroeck B, Sartor RB, Plevy SE. Altered macrophage function contributes to colitis in mice defective in the phosphoinositide-3 kinase subunit p110delta. *Gastroenterology.* 2010; 139:1642–1653. [PubMed: 20637203]
29. Arranz A, Doxaki C, Vergadi E, Martinez de la Torre Y, Vaporidi K, Lagoudaki ED, Ieronymaki E, Androulidaki A, Venihaki M, Margioris AN, Stathopoulos EN, Tschlis PN, Tsatsanis C. Akt1

- and Akt2 protein kinases differentially contribute to macrophage polarization. *Proc Natl Acad Sci U S A.* 2012; 109:9517–9522. [PubMed: 22647600]
30. Cao SS, Song B, Kaufman RJ. PKR protects colonic epithelium against colitis through the unfolded protein response and prosurvival signaling. *Inflamm Bowel Dis.* 2012; 18:1735–1742. [PubMed: 22275310]
 31. DeMeo MT, Mutlu EA, Keshavarzian A, Tobin MC. Intestinal permeation and gastrointestinal disease. *J Clin Gastroenterol.* 2002; 34:385–396. [PubMed: 11907349]
 32. Williams CS, Bradley AM, Chaturvedi R, Singh K, Piazuelo MB, Chen X, McDonough EM, Schwartz DA, Brown CT, Allaman MM, Coburn LA, Horst SN, Beaulieu DB, Choksi YA, Washington MK, Williams AD, Fisher MA, Zinkel SS, Peek RM Jr, Wilson KT, Hiebert SW. MTG16 contributes to colonic epithelial integrity in experimental colitis. *Gut.* 2013; 62:1446–1455. [PubMed: 22833394]
 33. Xiao H, Gulen MF, Qin J, Yao J, Bulek K, Kish D, Altuntas CZ, Wald D, Ma C, Zhou H, Tuohy VK, Fairchild RL, de la Motte C, Cua D, Vallance BA, Li X. The Toll-interleukin-1 receptor member SIGIRR regulates colonic epithelial homeostasis, inflammation, and tumorigenesis. *Immunity.* 2007; 26:461–475. [PubMed: 17398123]

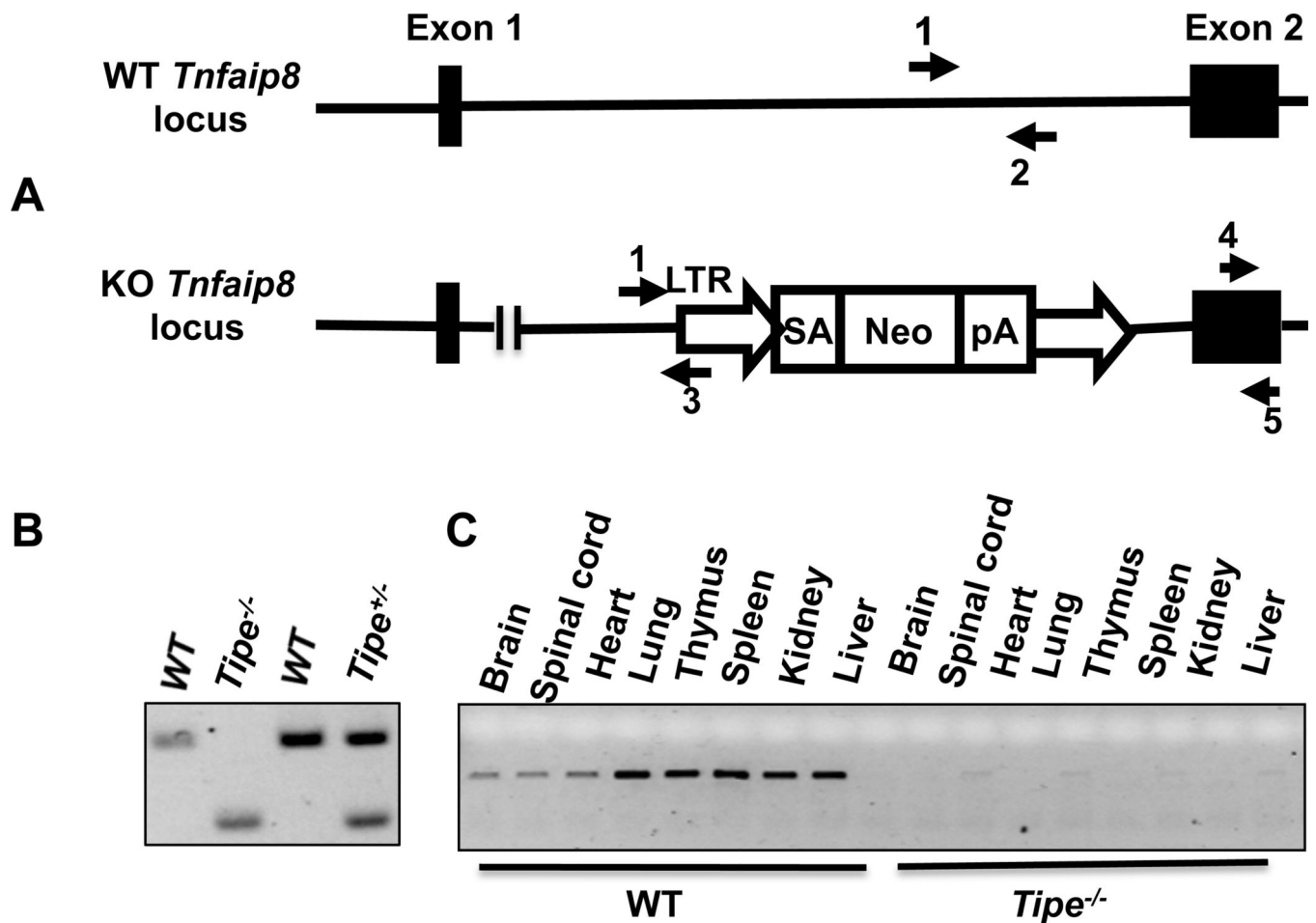


Figure 1. Generation of *Tipe*-deficient mice by gene targeting

(A) The wild-type *Tipe* (*Tnfaip8*) gene locus and the knockout allele. LTR: viral long terminal repeat; SA: splice acceptor; Neo: Neomycin-resistant gene; pA: poly adenylation sequence. Arrows indicate the locations of PCR primers. (B) Genomic DNA was extracted from mice tails. PCR was performed using primers shown in Panel A (primers 1, 2, and 3). WT band: 334 bp; *Tipe* knock out band: 190 bp. (C) Total RNA was isolated from the indicated organs of WT and *Tipe*^{-/-} mice; RT-PCR was performed using the *Tipe* primers shown in Panel A (primers 4 and 5).

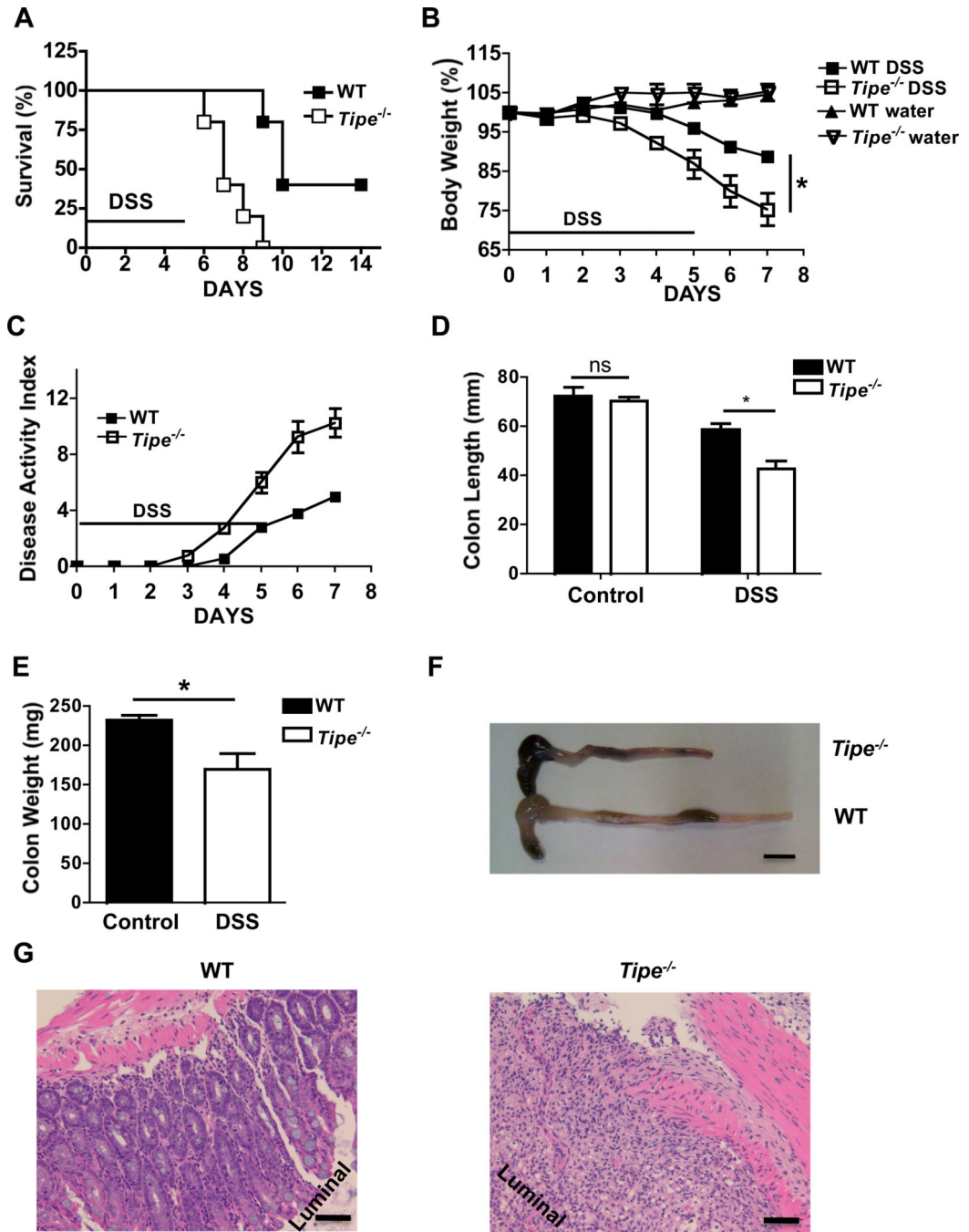


Figure 2. *Tipe*^{-/-} mice are more susceptible to DSS-induced colitis

(A) WT (n=5) and *Tipe*^{-/-} mice (n=5) were fed with DSS-containing water for five days, followed by regular drinking water. Survival was monitored for two weeks after the start of DSS treatment. (B-E) WT and *Tipe*^{-/-} mice were fed with DSS water for five days, followed by regular drinking water for two days. Body weight (B) and disease score (C) were recorded daily. On Day seven, mice were euthanized; colon length and weight (D, E, and F) were measured, and histopathological changes (G) in colon tissues were examined by

microscopy following H&E staining. Data shown are representatives of at least three experiments. Scale bar in 2F, 1 mm and in 2G, 50 μm . * $P < 0.05$.

Author Manuscript

Author Manuscript

Author Manuscript

Author Manuscript

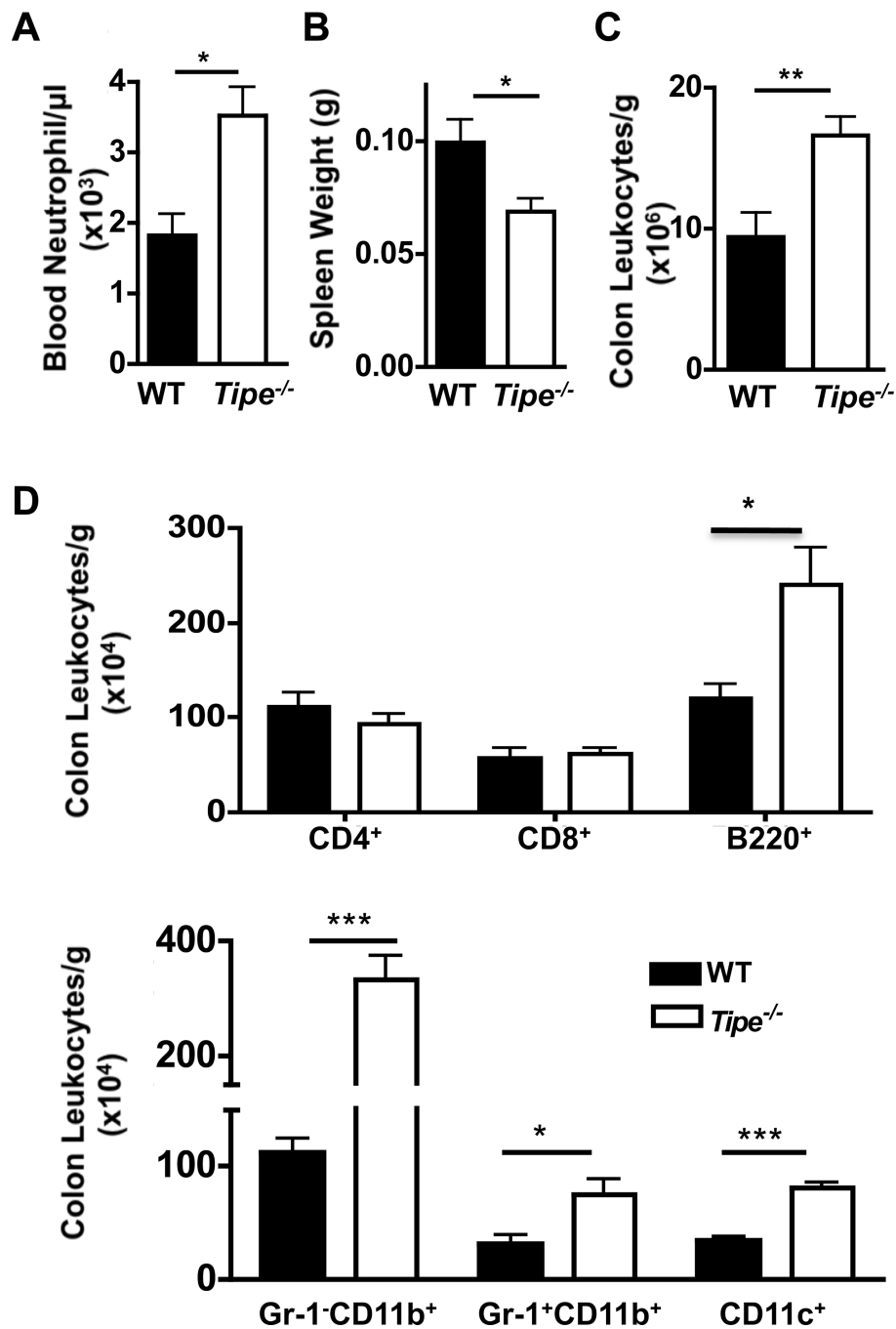


Figure 3. Increased leukocyte numbers in the blood and colon of *Tipe*^{-/-} mice
Mice (n=4) were treated and sacrificed as described in Figure 2. (A–B) Increased blood neutrophil counts (A) and decreased spleen weight (B) were detected in *Tipe*^{-/-} mice. (C and D) The colon from WT and *Tipe*^{-/-} mice were harvested and lamina propria immune cells were isolated. After counting in a hemacytometer, the cells were stained with antibodies to T, B, and myeloid cell markers, and analyzed by flow cytometry. Increased total (C) and CD11b, CD11c, and B220 cells (D) were identified. Data shown are representatives of at least three experiments. * $P < 0.05$; ** $P < 0.01$; *** $P < 0.001$.

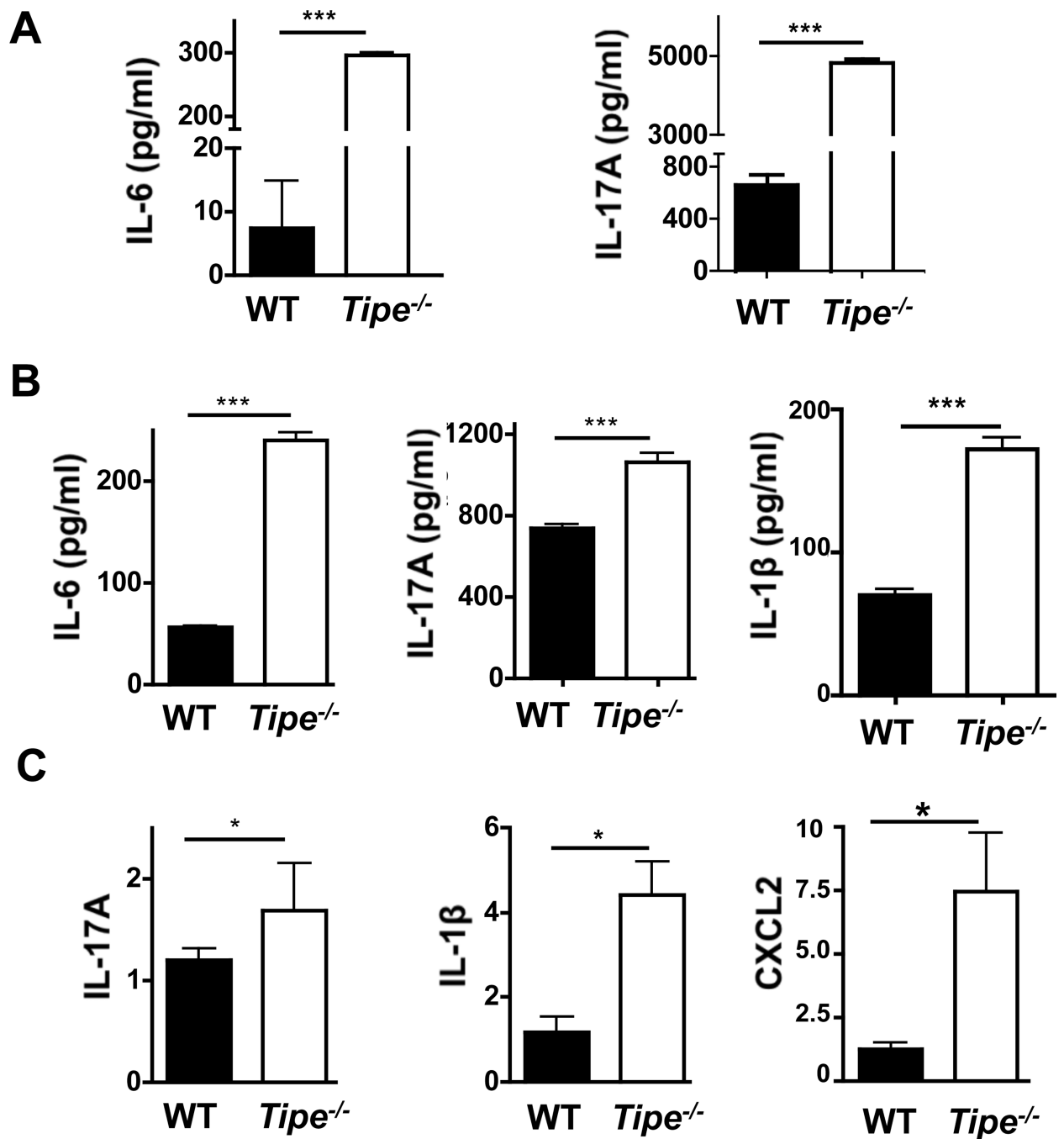


Figure 4. Increased inflammatory cytokines in serum and colon of *Tipe*^{-/-} mice

WT and *Tipe*^{-/-} (n=5) mice were treated with DSS water for five days, followed by regular drinking water for two days. Mice were then sacrificed, and their blood was collected retro-orbitally. Colons were harvested and ½ of them were homogenized in lysis buffer (weight/volume = 1/10). The cytokines in sera and colon homogenates were measured by ELISA. (A) IL-6 and IL-17 in sera. (B) IL-6, IL-17, and IL-1β in colon homogenates. (C) Total RNA was isolated from the other half of the colon using Trizol reagent. The levels of IL-17,

IL-1 β , and CXCL2 mRNAs were examined using quantitative real-time PCR. Data shown are representatives of two experiments. * $P < 0.05$; ** $P < 0.01$; *** $P < 0.001$.

Author Manuscript

Author Manuscript

Author Manuscript

Author Manuscript

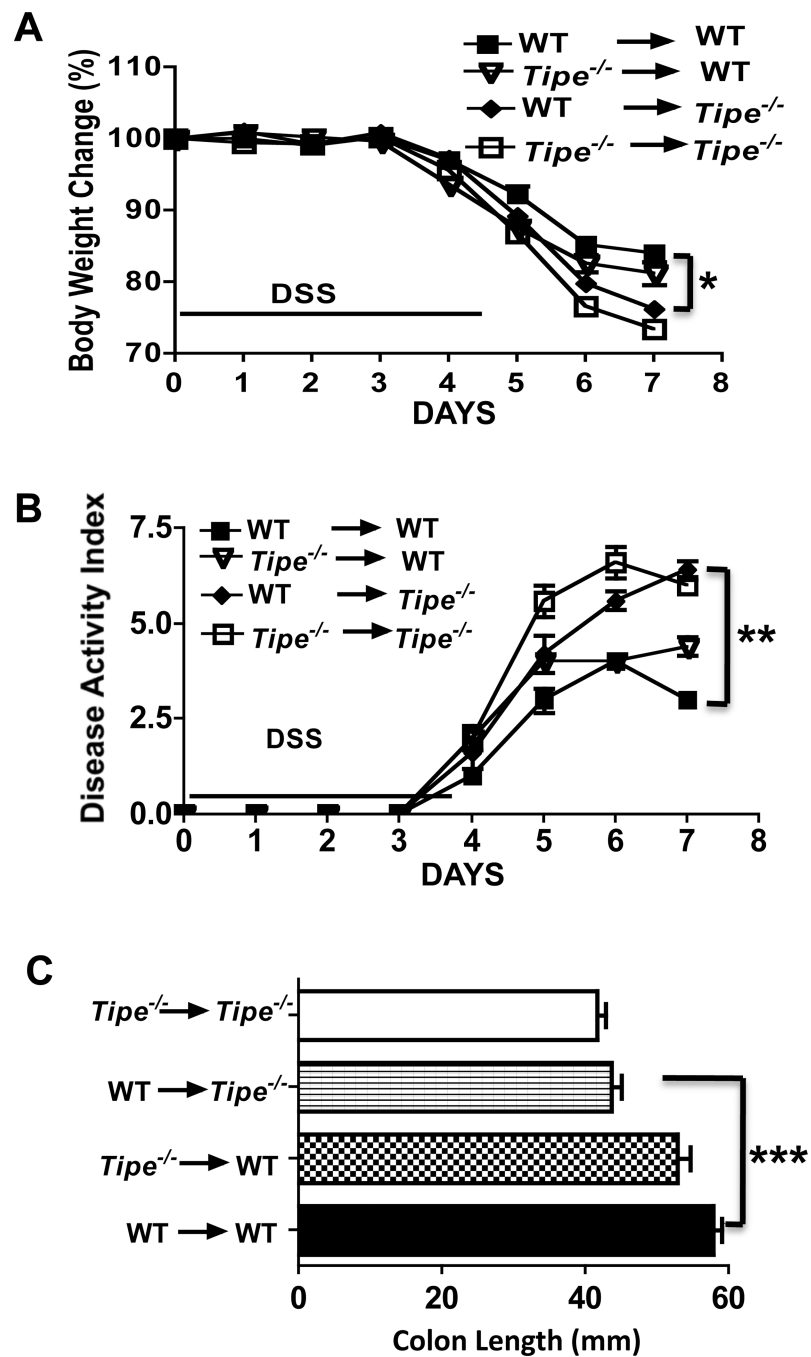


Figure 5. Tipe deficiency in non-hematopoietic cells contributes to the enhanced colitis in *Tipe*^{-/-} mice

Bone marrow chimeric mice (n=5) were generated as described in Methods and treated with DSS for five days, followed by regular drinking water for two days. (A) Body weight. (B) Disease activity index calculated based on the degrees of weight loss, stool consistency, and rectal bleeding. (C) Colon length. Data shown are representatives of two experiments.

* $P < 0.05$; ** $P < 0.01$; *** $P < 0.001$.

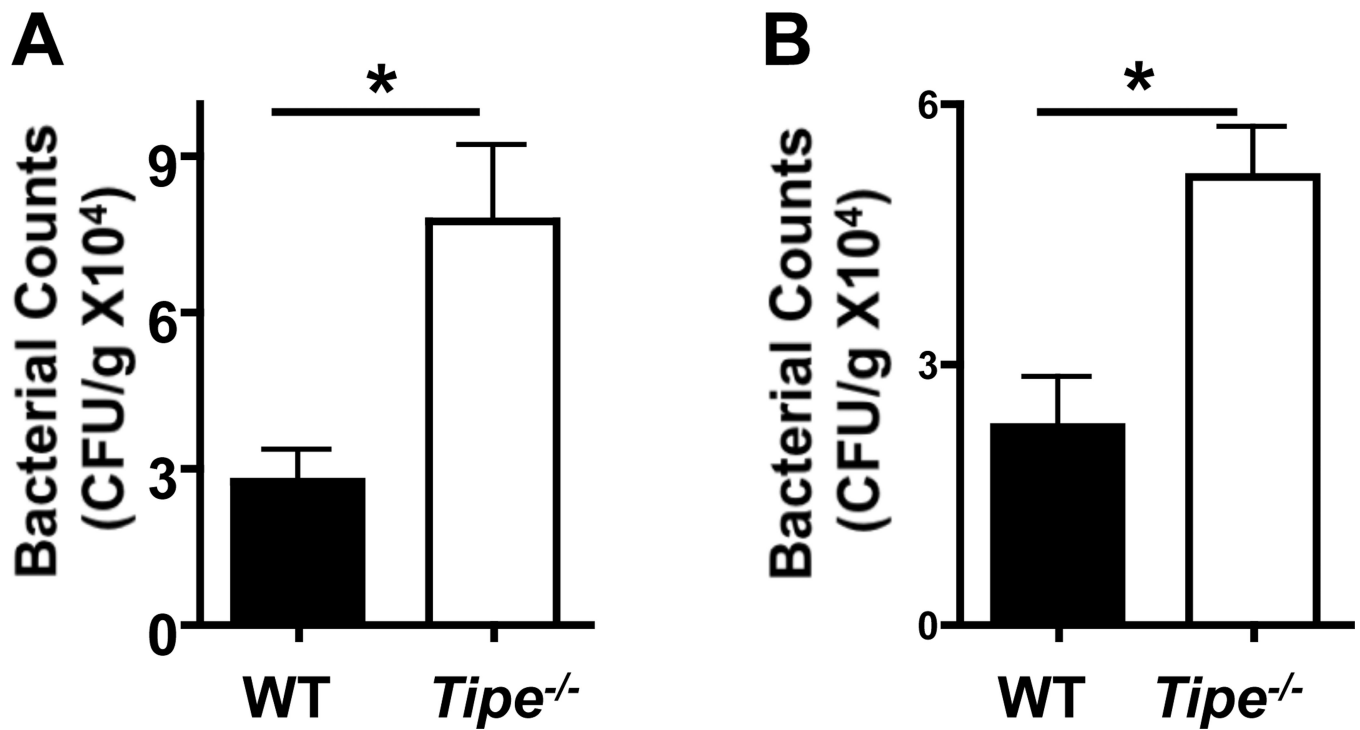


Figure 6. Increased bacterial invasion of *Tipe*^{-/-} colons

WT and *Tipe*^{-/-} mice (n=5) were fed with DSS for five days. Mice were then sacrificed and their colons collected. Colon homogenates were diluted and plated on blood agar (A) and BHI (B) plates for determining the bacterial counts. Data shown are representatives of two experiments. **P*<0.05.

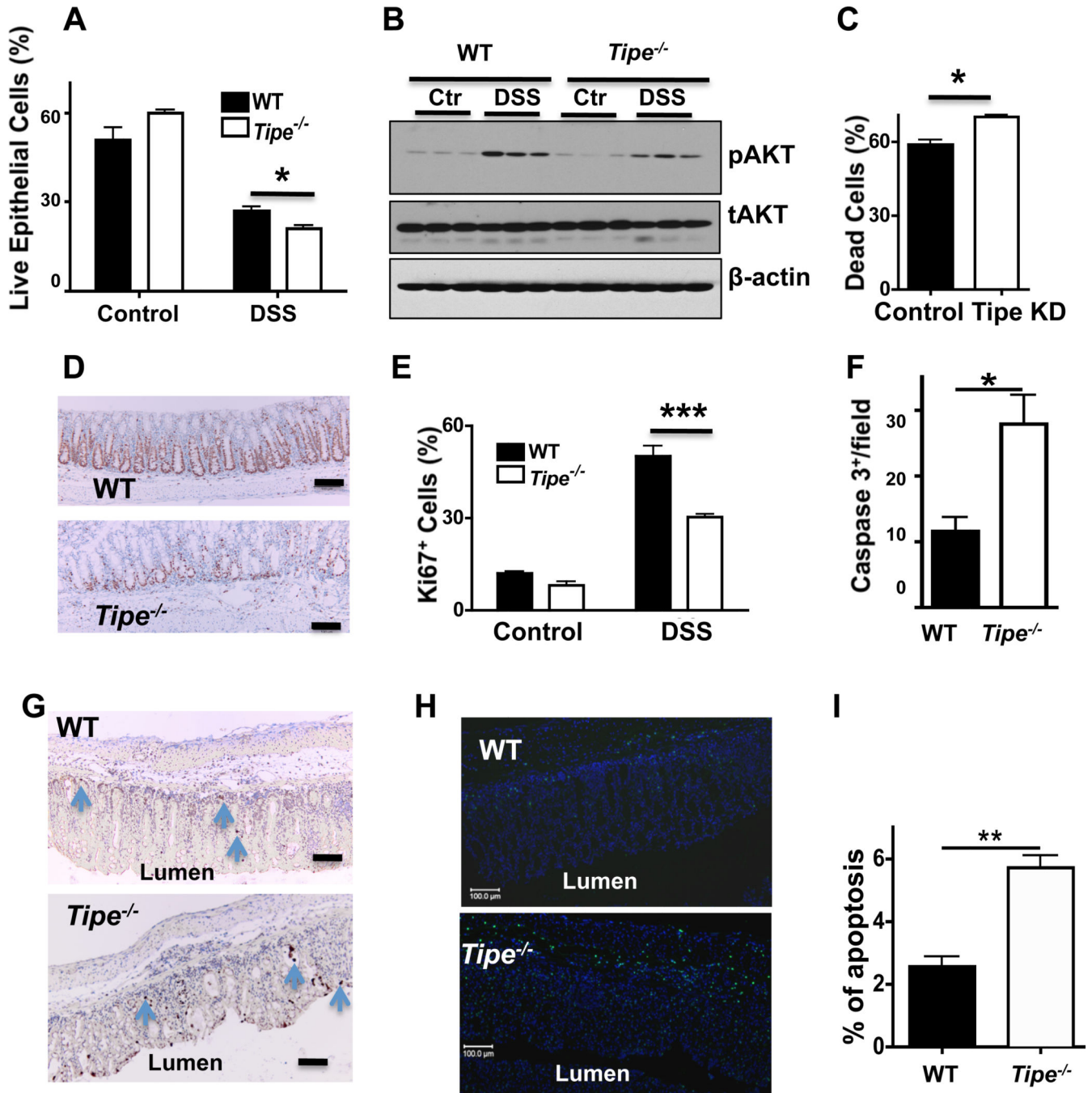


Figure 7. TIPE in gut epithelial cell death and growth, and AKT activation

(A) Mice were fed with or without DSS in drinking water for five days followed by regular drinking water for two days, and sacrificed as described in Figure 2. Epithelial cells from normal water-fed and DSS-fed WT and *Tipe*^{-/-} colons (n=5) were isolated and cell death was determined by 7AAD and Annexin V staining. Live cells were represented as 7AAD⁻ and Annexin V⁻. (B) Western blots for phospho-AKT (pAKT), total AKT (tAKT), and β-actin in WT and *Tipe*^{-/-} colon homogenates are shown. (C) NIH3T3 cells were transduced with shRNA-Tipe [Tipe knockdown (KD)] or shRNA-scramble (control), and treated with

3% DSS in culture medium for 16 hours. Cells were then collected and cell death was represented by Annexin V⁺ staining. (D) WT and *Tipe*^{-/-} mice were treated with DSS water for five days followed by regular drinking water for two days. Colons were collected, washed with cold PBS, fixed in formalin for 24 hours, sectioned, and stained with Ki67 antibody to measure colonic epithelial cell proliferation. (E) Bar graph shows percentages of Ki67⁺ cells in the colons of water-fed (control) and DSS-fed WT and *Tipe*^{-/-} mice. Scale bar, 100 μm. (F and G) WT and *Tipe*^{-/-} mice were treated as described in (D). Colons were collected at day 7, sectioned, and stained for active caspase 3 by immunohistochemistry. Data shown are numbers of active caspase 3⁺ cells per high power microscopic field (F) and representative images of colon sections with apoptotic cells shown in brown (G). At least six fields were counted for each sample. (H and I) Colon sections prepared as in (G) were stained by TUNEL and DAPI. The representative TUNEL positive (green) and DAPI positive (blue) cells are shown (H). Bar graph shows the percentage of TUNEL positive cells from at least six fields per sample (I). **P*<0.05; ***P*<0.01; *** *p*<0.001. Data shown are representatives of two experiments.

Author Manuscript

Author Manuscript

Author Manuscript

Author Manuscript